Microbial two front attack: elaborate root infections by *Colletotrichum graminicola* oval conidia during maize anthracnose

Rudolph A. Y.[1], Schunke C.[1],Sasse C.[2], Antelo L.[3], Gerke J.[2], Braus G.[2], Pöggeler S.[1], Nordzieke D.E.[1,*]

[1]University of Göttingen, GZMB, Institute of Microbiology and Genetics, Genetics of Eukaryotic Microorganisms, Grisebachstr. 8, 37077 Göttingen, Germany; dnordzi@gwdg.de

[2]University of Göttingen, GZMB, Institute of Microbiology and Genetics, Microbiology and Genetics, Grisebachstr. 8, 37077 Göttingen, Germany

[3]Johannes Gutenberg-University of Mainz, Institute of Molecular Physiology, Microbiology and Biotechnology, Hanns-Dieter-Hüsch-Weg 17, D-55128 Mainz, Germany

Current address Carolin Schunke:

Ruprecht Karls Universität Heidelberg, Heidelberg University Biochemistry Center (BZH), Im Neuenheimer Feld 328; 69120 Heidelberg, Baden-Württemberg, Germany

Current address Jennifer Gerke:

Leibniz Universität Hannover, Institute for Organic Chemistry, Biomolekulares Wirkstoffzentrum, Schneiderberg 38, 30167 Hannover, Germany

*Correspondence: dnordzi@gwdg.de

Abstract

Most plant pathogenic microorganisms have evolved to infect distinct host tissues. The maize anthracnose fungus, *Colletotrichum graminicola*, is known for its ability to invade above-ground tissues with asexual falcate conidia. Besides, *C. graminicola* generates a second asexual spore type, oval conidia. We analyzed in this study specific adaptations making oval or falcate conidia prone for maize root infection, providing evidence that only oval conidia show characteristics of a root pathogen. This includes the ability to germinate in soil and to grow chemotropically toward root-secreted molecules. HPLC/MS analyses combined with biological assays revealed that diterpenoids like dihydrotanshinone I are most likely responsible for the chemical attraction of *C. graminicola*. A genetics approach identified the a-pheromone receptor CgSte3 as being responsible for the perception of diterpenoids by the fungal pathogen. In conclusion, the understanding of the maize anthracnose disease has to be expanded to include an elaborated root infection cycle by oval conidia.

Introduction

The health of crop plants and fruits is affected by different organism groups, ranging from viruses, microorganisms (bacteria, oomycetes, fungi) to complex eukaryotes (nematodes, parasitic plants)[1]. Among those, fungi stand out as pathogens of the main crops for food production, reducing the yield and quality of agricultural production by the destruction of plants

(preharvest) and their fruits (postharvest)[2,3]. Timely precise and sustainable crop protection strategies are required, especially since the burden of fungal plant diseases are predicted to shift due to climate change[4,5].

Fungal plant pathogens are specialized on entering their host plant via distinct tissues (roots, shoots, stems, stalks, leaves) or at distinct developmental stages (flower, fruit). Depending on the infected tissue, adapted signal sensing machineries and infection strategies are required. Foliar pathogens sense the plant surface via its physical and chemical properties, inducing the germination and pathogenicity program of the fungus[6]. In contrast, fungal root pathogens do start their infection process before being in direct contact with the host. Sensing of nearby (host-) plants by root exudates initiate germination of resting structures and directed growth towards plant-secreted signals (chemotropism)[7-10]. The known chemical signals for this directed growth response include sugars, amino acids, organic acids, fatty acids and plant-derived enzymes like peroxidases. These molecules guide pathogens like *Fusarium oxysporum*, *Fusarium graminearum* and *Verticillium dahliae* to the roots of their hosts[11-17], where they start root surface colonization and host invasion[18,19]. Additionally, some fungi like *Magnaporthe oryzae* predominantly known as leaf pathogens are able to infect root tissues, at least under laboratory conditions, by direct treatment of roots by conidia suspensions or mycelial plugs[20,21].

The hemibiotrophic maize pathogen *Colletotrichum graminicola* is known mainly for its ability to infect above ground tissues like leaves and stems[22]. Current analyses estimate that only due to the anthracnose stalk rot (ASR), 10-20% of the maize harvest is lost worldwide annually[23,24]. Like other relevant plant pathogens, *C. graminicola* generates two different types of asexual spores, namely oval and falcate conidia. In contrast to micro- and macroconidia in other fungal pathogens, both spore types are metabolically active and generated via different developmental processes in distinct plant tissues[25-27]. Falcate conidia develop in acervuli, asexual fruiting bodies, in a controlled process on infected leaves. The hallmark of acervuli are setae, dark spike-like hyphae, surrounded by huge masses of falcate spores. Oval conidia, however, pinch off from hyphae in the plant's vascular system and are stored in parenchyma cells of the plant[24,28]. Those specifications influence the morphological and physiological properties of both spore types. Falcate conidia have only one nucleus and are dormant by the generation of mycosporines, self-inhibitors of germination. In contrast, the formation process of oval conidia is rather uncontrolled and resembles hyphal branch formation[27,29]. Therefore, oval conidia contain a variable number of nuclei and secondary metabolites promoting dormancy are absent. Those differences cumulate in distinct leaf infection strategies for both conidia types as we reported previously[29,30]. Together, these findings imply so far unexplored but specific roles of both spore types in the maize anthracnose cycle.

This study provides the first comparative study between the root infection potentials of both *C. graminicola* spore types. As main findings, our analyses revealed that only oval conidia show the distinct characteristics of a fungal root pathogen. Only oval conidia are adapted to germinate and propagate in soil and grow chemotropically towards maize root exudates. Thus, they are able to cause disease symptoms under natural infection conditions. We found strong indications that maize root-secreted diterpenoids act as attractants for the chemotropic growth by a combination of chemical analysis and biological activity assays. The *C. graminicola* a-mating type pheromone receptor Ste3 was identified as diterpenoid sensor of this elaborate host detection system. Our results support that under natural field conditions oval conidia are better adapted to root infection. As the major critical difference between both spore types, the ability to germinate in soil was identified. In summary, we describe for the first time how the

generation of a second spore type allows a fungal plant pathogen to efficiently infect a host by several plant tissues.

Results

Root dipping in *C. graminicola* oval conidia induce a symptomless maize root infection and disease spreading into maize stems

C. graminicola is the causal agent of maize anthracnose and generates two types of asexual spores. Falcate conidia are more efficiently causing anthracnose leaf blight (ALB)[29] and had been described earlier to infect roots[28]. In this study, the general abilities of both spore types to colonize the root surface and to spread within the host was compared. A *C. graminicola* wildtype strain expressing a tdTomato-labelled histone marker, CgM2::RH2B[29], enabling the easy detection of the growing fungus on the surface of the root, was analyzed. CgM2::RH2B oval or falcate conidia suspensions were used as inoculum for the infection of 5 d old maize roots prior to incubation under humid conditions. The microscopic evaluation shows production of several fungal structures as previously observed for root infection with falcate conidia[28]. At 4 d post infection, production of acervuli, the asexual fruiting bodies, was observed for both conidia types (Figure 1). Additionally, development of typical root colonization structures like long, fast growing runner hyphae, hyphopodia for root penetration and dark-pigmented resting structures (microsclerotia) were observed upon oval and falcate conidia colonialization (Figure S1).

5 d old plants dipped in conidial suspensions were planted out in vermiculite to analyze symptom development on the growing plant. After 21 d of growth under humid conditions, length and biomass of above ground tissue was measured. As depicted in Figure S 2, no significant differences to mock inoculation were observed. A probable symptomless systemic infection was verified by taking stem samples as basis to detect fungal biomass in the respective plants in a real-time PCR approach. Specific detection of *C. graminicola* was ensured by the design of oligonucleotides binding in the species-specific region of ITS1 and ITS2 (Figure S3 and S4). In 50% of plants infected with oval conidia fungal biomass was detected in stem material, whereas *C. graminicola* gDNA was absent in plants treated with falcate conidia (Figure 1 C). This supports a more effective *in planta* growth outgoing of oval conidia infection.

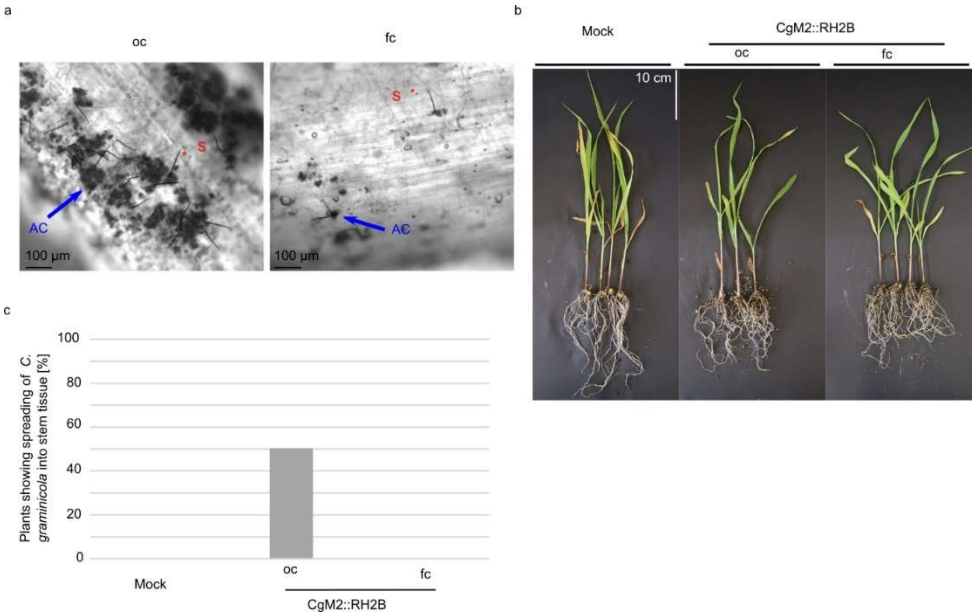

Fig 1: **Symptom development after dipping root infection of *Z. mays* with *C. graminicola*.** (a-c) Roots of 5 d old plants were dipped in oval (oc) or falcate (fc) conidial suspensions of CgM2::RH2B allowing for the detection of red-fluorescent nuclei during microscopic visualization. (a) *C. graminicola* development on roots 4 d after root dipping, AC = acervulus (blue arrow), S = setae (red asterisk), scale bar = 100 µm. (b-c) Symptom development 21 d after root dipping in conidial suspensions. Growth in vermiculite. (b) Representative depiction of plant development, scale bar = 10 cm. (c) Quantification of plants with spreading of *C. graminicola* in stem tissue by real-time PCR.

Maize root exudate and diterpenoids elicit a strong chemotropic response by germlings derived from oval conidia

Directed growth to plant-secreted signals was described for several root-infecting pathogenic fungi[15,16,31]. The amount of germlings derived from oval and falcate conidia, which are able to redirect growth towards maize root-secreted signals, was quantified. A 3D printed device was applied for quantification, which was recently developed in our laboratory[32]. Oval conidia are well germinated after 6 h of incubation. They show typical localization of the polarity marker CgArp1-TagRFP-T[33] to the subapical region of growing hyphae. The corresponding hyphal tips point mainly to the gradient of maize root exudate (MRE), indicating active hyphal growth of the germlings to the root-secreted signals (Figure 2 a, b). In contrast, we were unable to detect any germinated falcate conidia, indicating that those spores are unable to germinate and redirect growth under the experimental conditions (Figure 2 a).

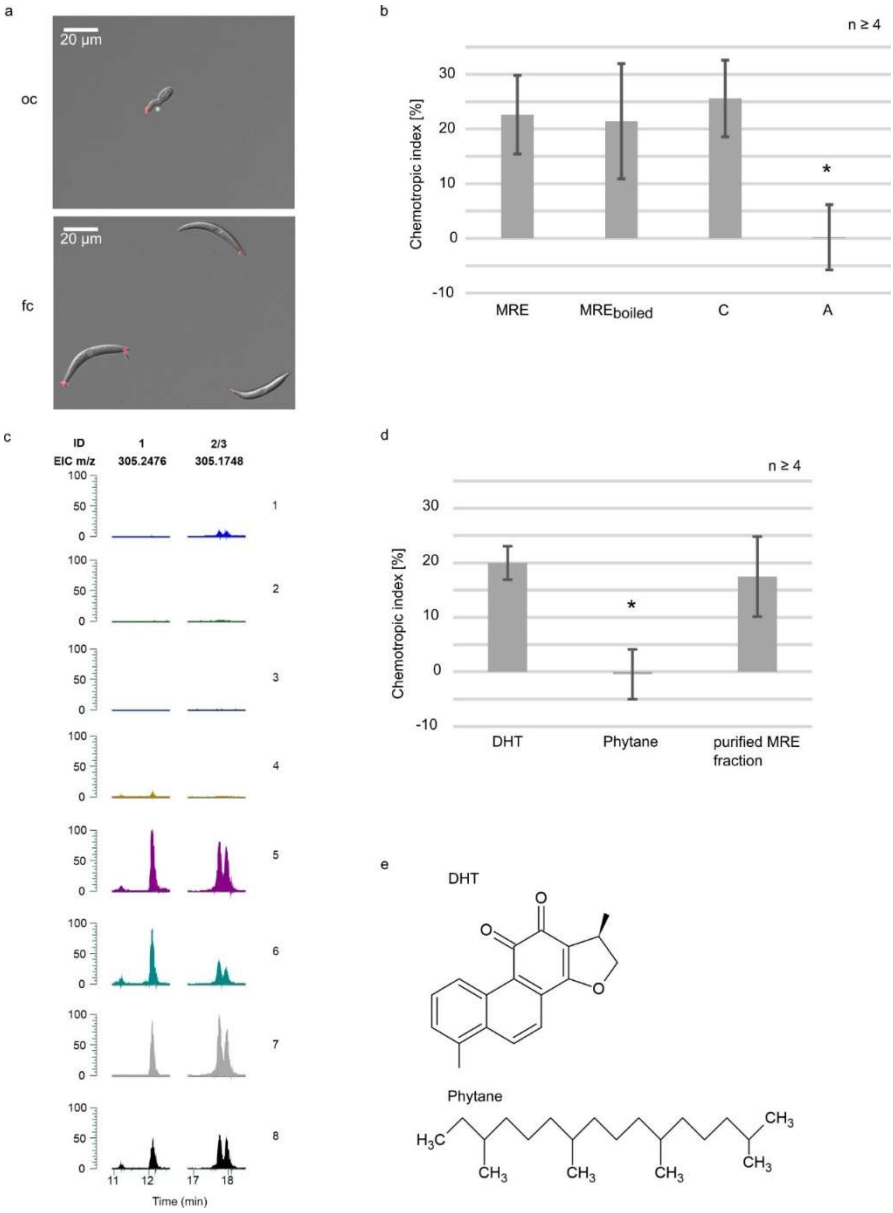

Fig 2**: Chemotropic growth of *C. graminicola* conidia.** (a) oval and falcate conidia of *C. graminicola* expressing red-labeled Arp1 (CgM2::Arp1-TagRFP-T, [33]) after 6 h of incubation facing a gradient of maize root exudate (MRE). Germination is indicated by a white asterisk, scale bar = 20 µm. (b) Chemotropic index of CgM2 oval conidia facing gradients of different chemoattractants including MRE and boiled MRE. Chloroform (C) and aqueous (A) phases gained from lipid extraction (chloroform:methanol) of MRE. Error bars represent SD calculated from n ≥ 4 experiments, * $p < 0.05$. (c) HPLC/MS analyses of non-attracting (fractions 1-4) and attracting (fractions 5-8) MRE fractions. Extracted Ion Chromatograms (EICs) for the identified metabolites 1 und 2/3. m/z 1 was detected in positive mode. ID (number of the compound in this study). The samples were extracted with ethyl acetate (1:1) or chloroform:methanol (1.8:2.2), n ≥ 2. Fractions: 1 = demineralized water; 2 = demineralized water used as basis for a chloroform:methanol extraction, chloroform phase; 3 = demineralized water used as basis for a chloroform:methanol extraction, aqueous phase; 4= MRE used as basis for chlorform:methanol extraction, aqueous phase; 5 = MRE after ethylacetate extraction; 6 = MRE boiled after ethyl acetate extraction; 7 = MRE used as basis for chloroform:methanol extraction, chloroform phase; 8 = MRE obtained from *C. graminicola* root-infected plants. (d) Chemotropic growth of *C. graminicola* oval conidia towards different chemoattractants. Error bars represent SD calculated from n ≥ 4 experiments, * $p < 0.05$, calculated with two-tailed *t*-test (e) Chemical structure of the tricyclic diterpenoid dihydrotanshinone I (DHT) and phytane, a linear diterpenoid. Chemical structures drawn with ACD/ChemSketch.

163 Next, we sought to identify the attracting molecule incorporated in MRE. Secreted peroxidases
164 from the host were identified as chemoattractant signals in plant interaction studies with other
165 phytopathogenic species[15-17]. Since the enzymatic activity of those enzymes are required for
166 fungal attraction, boiling of tomato root exudate abolishes its attracting potential[15,31]. In
167 contrast, boiling of MRE does not diminish the chemotropic growth index of *C. graminicola*
168 germlings (Figure 2 b), indicating that peroxidases are not the attractant secreted from maize
169 roots. Chloroform / methanol extractions were performed to explore further chemical properties
170 of the active MRE, resulting in two phases with different chemical properties. Intriguingly, the
171 chloroform phase, incorporating unipolar compounds such as lipids or lipid-associated
172 molecules, induced a strong chemotropic response after solvent evaporation and
173 resuspension in water. No directed growth was induced by the water phase typically containing
174 nucleic acids (Figure 2 b). Attracting (MRE, boiled MRE, MRE chloroform phase of lipid
175 extraction, MRE obtained from *C. graminicola* infected plants) and not attracting
176 (demineralized water and its chloroform and aqueous phase of lipid extraction, MRE aqueous
177 phase of lipid extraction) samples were compared using HPLC / MS analyses. Exudates
178 generated from previously root-infected plants were also included, to test whether previous
179 biotic stress by *C. graminicola* root infection might change the chemical composition of the
180 MRE. Three molecules in the active fractions were consistently detected in three independent
181 experiments, at the same time absent from the negative controls (Figure 2 c, Figure S5).
182 Interestingly, the double peak eluting at approximately 18 min was absent in the third replicate,
183 except for the MRE sample from *C. graminicola* root infected plants. This indicates a flexibility
184 of MRE composition dependent on the defense status of the plant. Comparing UV and MS2
185 spectra of the chemical compound released at 12 min (mass: 305,2476) with known
186 diterpenoids from maize, we found the colorless 3β,15,16-trihydroxydolabrene
187 (trihydroxydolabrene, THD) having a very similar MS2 spectrum (Figure S6)[34]. After
188 fractionation of this single peak, we verified its attracting potential in a chemotropic assay
189 (Figure 2 d). We conclude it as very likely that the maize root-derived diterpenoid THD is
190 attracting *C. graminicola* oval conidia to its host. In order to test non-maize diterpenoids for
191 their attracting potential, we chose dihydrotanshinone I (DHT, originated from *Salvia* species),
192 a cyclic diterpenoid like THD, and phytane, a linear diterpenoid. As depicted in Figure 2 d-e,
193 oval conidia of *C. graminicola* are attraced by DHT. In contrast, the linear diterpenoid phytane
194 did not induce a re-direction of *C. graminicola* germlings.

195

196 The CgSte3 a-pheromone receptor is responsible for diterpenoid sensing in *C. graminicola*

197 In different *Fusarium* species, the pheromone receptors Ste2 (α-pheromone receptor) and
198 Ste3 (a-pheromone receptor) activate the downstream Cell Wall Integrity (CWI) MAPK
199 cascade, resulting in the re-direction of growth towards plant-derived peroxidases[15,16,35]. In
200 contrast to other filamentous fungi, *C. graminicola* does not encode a *ste2* gene and the
201 corresponding α-pheromone is likewise missing in the genome[36]. Therefore, a *Cgste3* deletion
202 mutant was generated and characterized to test whether homologous pathway components
203 are responsible for diterpenoid sensing by *C. graminicola* (Figure S7 and S8). Intriguingly,
204 germlings derived from ΔCgste3 oval conidia are unable to re-direct their growth to MRE and
205 DHT (Figure 3 a), providing evidence that this receptor is required for the sensing of diterpenoid
206 plant signals by *C. graminicola*.

207

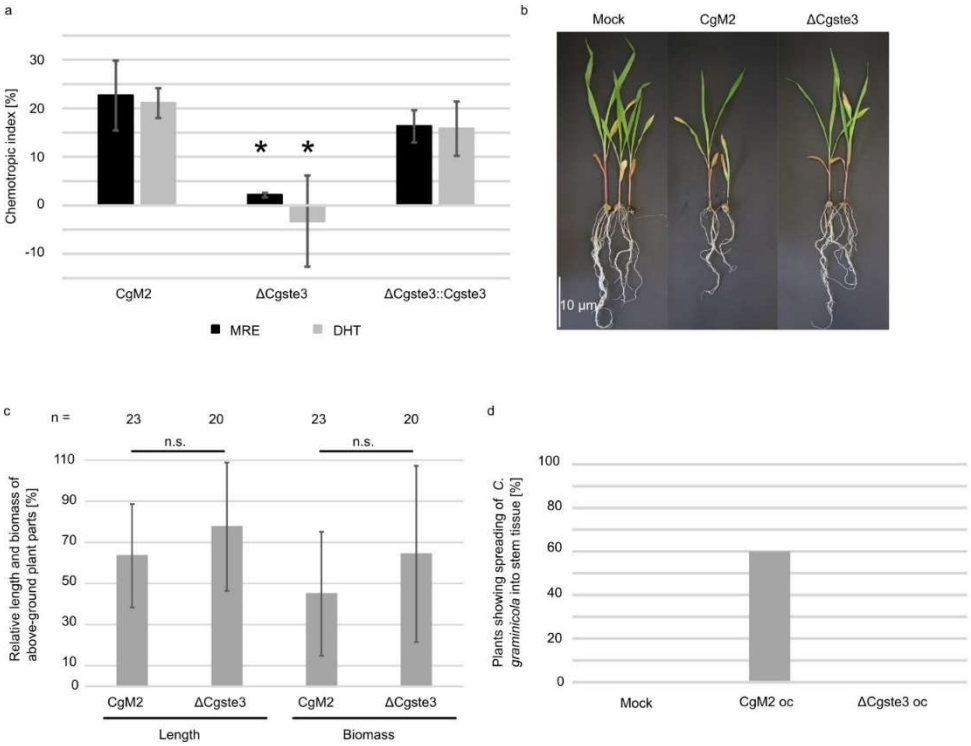

Fig 3: **Perception of maize diterpenoids by a conserved fungal signaling pathway.** (a) Chemotropic index of CgM2, Cgste3, and Cgste3::Cgste3 oval conidia facing gradients of different chemoattractants including MRE and dihydrotanshinone I (DHT). Statistical significance was calculated with CgM2 as reference. (b-c) Symptom development of plants co-incubated with conidia in vermiculite. (b) Representative depiction of plant development, scale bar = 10 cm. (c) Quantification of length and biomass of above-ground parts. Error bars represent SD calculated from n ≥ 20 experiments, ns = not significant. Statistical significance was calculated with two-tailed *t*-tests (d) Quantification of plants with spreading of *C. graminicola* in stem tissue with real-time PCR.

As many studies reported, spores of plant pathogenic fungi are adapted to germinate in the presence of an adequate host and to direct their growth towards its roots[8,15,17,37,38]. Maize seeds were disseminated in oval conidia-enriched soil of the *C. graminicola* wildtype strain CgM2 to mimic this natural infection situation under laboratory conditions (Figure 3). After three weeks of co-incubation, length and biomass of green plant parts were examined (Figure 3 b-c). In contrast to the results obtained by root-dipping, oval conidia co-incubated maize plants are significantly stunted and reduced in biomass compared to mock treatment and on some leaves typical anthracnose symptoms occurred (Figure S9). Experiments outgoing from spore-enriched soil were also conducted with the mutant strain of ΔCgste3 (Figure 3 c-d). However, no difference between ΔCgste3 infections to wildtype was observed. To compare *in planta* growth between the wildtype and mutant strain, stem samples were used to detect of fungal biomass in a real-time PCR approach as described above. Whereas fungal DNA was present in 50% of plants co-incubated with oval conidia of the wildtype, oval conidia of the *Cgste3* deletion mutant did not spread into stem tissue (Figure 3 d).

Successful germination of *C. graminicola* conidia in soil determines the ability to infect maize roots

Besides the ability to re-direct growth to MRE, one of the most prominent differences between oval and falcate conidia are the specific germination patterns. Germination of falcate conidia

236 is regulated by a quorum sensing mechanism based on the secretion of mycosporines. In
237 contrast, oval conidia do not secrete mycosporine-derivatives and thus germinate rapidly even
238 when nutrients are absent[29]. These spore-type specific adaptations suggested that there might
239 be divergent germination patterns in vermiculite or other plant substrates, which influence the
240 abilities of both spore types to infect the host plant's roots.

241 The germination ability of oval and falcate conidia in soil of different compositions was analyzed
242 to address this hypothesis (Figure 4 a, b). After incubation, the spore-contaminated soil was
243 washed with a defined amount of water. The number of not germinated spores washed out
244 was determined, assuming that germinating conidia would stick to the pieces of substrate.
245 Independent of the substrate used, the fraction of non-germinated oval conidia dropped down
246 already after 6 h of incubation (vermiculite: 75% reduction; vermiculite soil mix: 43.8%
247 reduction). The number of oval conidia increased within the first two days of inoculation in both
248 substrates. Although this effect was more pronounced in the vermiculite soil mix, a probable
249 formation of new spores in the watered substrates is indicated. The main fractions of conidia
250 were germinated in both spore samples after 10 d of incubation (vermiculite: 62% reduction;
251 vermiculite soil mix: 92.8% reduction). In contrast, for falcate conidia the amount of not
252 germinated spores detected remained stable, also after prolonged incubation for 10 d.

253 It was shown for several root-interacting fungi that root exudate could induce germination[8,37,38].
254 We thus tested whether MRE is able to induce germination of falcate conidia on axenic culture
255 or in soil. For the first experiments, defined drops of falcate conidia were incubated on water
256 agar with or without the addition of MRE. As depicted in Figure 4 c, MRE was unable to induce
257 germination in falcate conidia. We further analyzed the effect of living maize plants on the
258 germination ability. Consistently to the previous results, only non-germinated falcate conidia
259 were detectable after 10 d of plant-co-incubation (Figure 4 d). Furthermore, many highly
260 vacuolated and dead falcate conidia were detected, indicating that this spore type is unable to
261 survive for a longer time in soil (Figure S10).

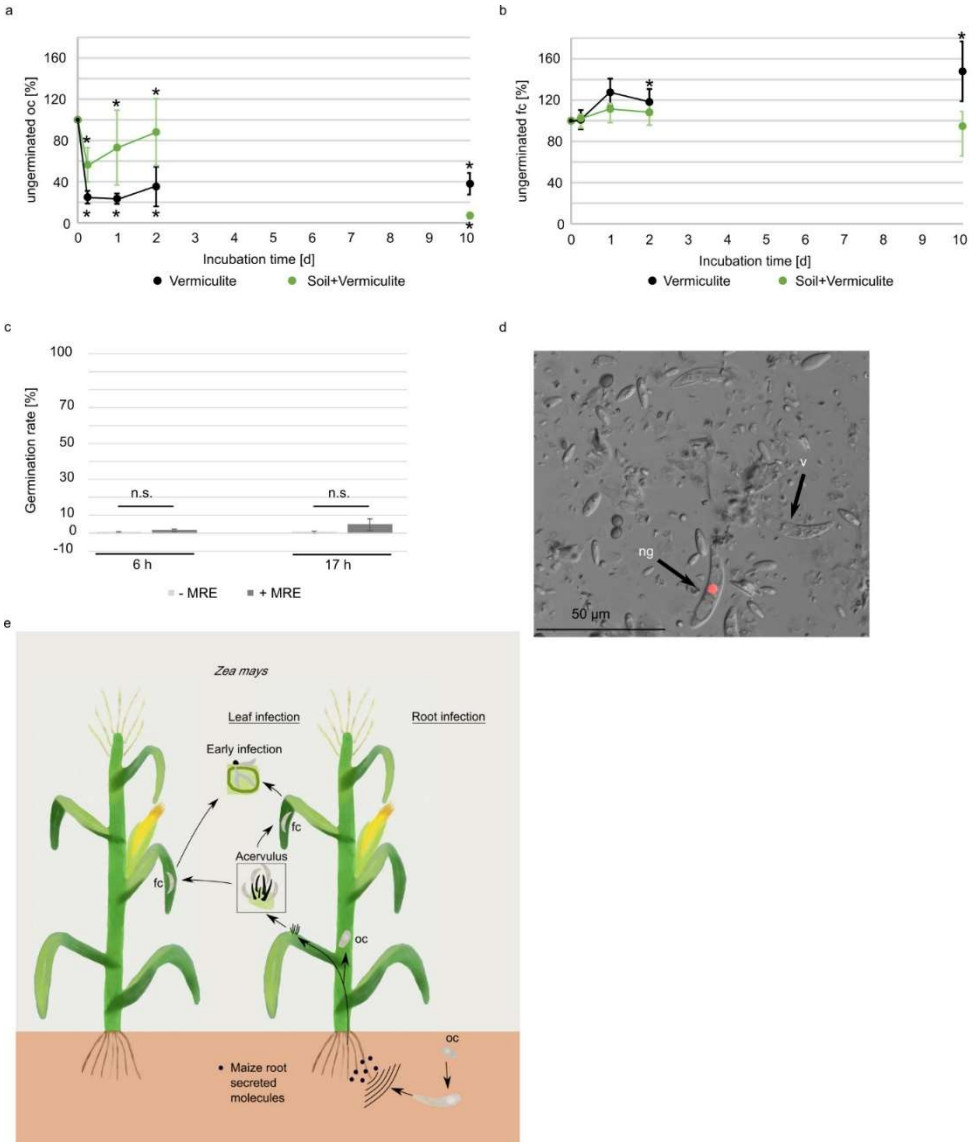

Fig 4: **Germination of *C. graminicola* conidia.** (a, b) Germination of oval (oc) (a) and falcate (fc) (b) conidia in vermiculite and a mixture of soil and vermiculite (4+1). Quantification of ungerminated conidia after incubation of 0 h, 6 h, 24 h, 48 h, 10 d in a Neubauer counting chamber. (c) Germination of falcate conidia (fc) on water agar after 6 h and 17 h with and without the supplement of MRE. Two-tailed t-tests were performed. * $p < 0.05$, n.s = not significant. (d) Falcate conidia (black arrows) in soil after a 10 d co-incubation with maize roots in vermiculite, ng = not germinated, scale bar = 50 µm (e) Model of the maize infection cycle. In the monocyclic part, oc of *C. graminicola* germinate in soil and grow chemotropically towards plant-secreted molecules. The fungus penetrates roots and systemically infects the plant leading to fc production in acervuli on leaves. Spreading of fc to nearby plants starts the polycyclic disease cycle. Leaf infection starts with inoculum and adhesion of spores, followed by development of the penetration structures.

Discussion

The phytopathogenic fungus *Colletotrichum graminicola* produces two distinct asexual spore types. The main finding of this study is that only oval conidia are adapted for the infection of maize roots, whereas the falcate asexual spores invade above ground tissues. This has two major reasons: only the oval conidia have the ability for fast germination in soil and they can efficiently sense maize root exudates, which provide growth orientation towards the host.

280 These findings shed new light to the more complex overall maize anthracnose cycle and
281 provide important implications for future crop protection strategies (Figure 4 e).

282 Exudates from plant roots fulfill several important functions for plant health like the adaptation
283 of soil pH to increase nutrient intake, chelation of toxic compounds, attraction of beneficial
284 microorganisms and the release of antimicrobial substances for the defense against
285 pathogens[10,39]. During attack, plants additionally adapt the composition of root exudates by the
286 *de novo* biosynthesis of compounds with antimicrobial functions[40]. Prominent examples of
287 such antimicrobial compounds are class III peroxidases secreted from plant roots, taking part
288 in reactive oxygen species defense pathways[41-43]. However, several pathogenic fungi are able
289 to sense those peroxidases and – instead of harming or chasing away – these enzymes are
290 guiding the pathogens towards nearby (host) plants by an elaborated amplification and sensing
291 system involving fungal NADPH oxidase and pheromone receptors[15-17,31]. In this present study,
292 we describe for the first time the ability of *C. graminicola* oval conidia to sense root exudates
293 of maize, provoking a robust chemotropic response. Chemical analysis and fractionation
294 experiments revealed that the active substances secreted from maize roots are heat-stable
295 and soluble in chloroform (Figure 2). Comparisons of the masses gained from HPLC/MS
296 analysis with known secondary metabolites showed a high similarity with diterpenoids. UV and
297 MS2 spectra of one compound has a good overlap with 3β,15,16-trihydroxydolabrene
298 (trihydroxydolabrene, THD). This colorless diterpenoid is secreted from maize roots and has
299 antimicrobial functions[34]. Diterpenoids are described to take part in terpenoid-based defenses
300 against various maize pathogenic species, including the fungi *Rhizopus microsporus*, *Ustilago*
301 *maydis*, or *F. graminearum* but also herbivorous and insect species[44]. Similar to findings
302 regarding class III peroxidases, the biosynthesis of several deterpenoids is inducible by plant
303 pathogens as well as defense-related phytohormons jasmonic acid and ethylene[45-48]. Our
304 results show that diterpenoid and MRE perception in *C. graminicola* is routed by the a-
305 pheromone receptor Ste3, indicating a certain level of conservation in the sensing of host-
306 secreted molecules despite the different chemical properties of the attractants[15-17]. However,
307 and in contrast to *Fusarium* and *Verticillum* species, the absence of the α-pheromone receptor
308 Ste2[36] seems not to hamper the perception of maize root secreted signals, indicating
309 differences in the perception process despite their similarities. Together, these results indicate
310 that the ability to use plant defense molecules for host detection occurred several times during
311 evolution and is adaptable to different chemical compounds dependent on the fungal-plant
312 pathosystem involved.

313 An important question is the relevance of chemotropic sensing by *C. graminicola* oval conidia
314 and derived germlings for the adaptation of this spore type for maize root infection. From our
315 experimental data, we conclude that chemotropic sensing of maize root exudates is not
316 essential for the *C. graminicola* root infection process *per se*, but might have a variable impact
317 on the overall process depending on the spore concentration in the proximity of the young
318 maize plant. In a high inoculum scenario, it might be sufficient to be exposed to *C. graminicola*
319 germinated oval conidia, which accidently find the roots of nearby maize plants. Consequently,
320 the infection process, although delayed, might take place, mirrored by a retarded spreading of
321 *C. graminicola* inside the host. In field conditions however, low spore inocula of one species
322 are probable, bestowing a high relevance for the chemotropic guidance of the pathogen to its
323 host. This study underlines the high relevance of adequate germination for plant infection.
324 Falcate but not oval conidia generate mycosporines, self-inhibitors of germination, generated
325 at high spore densities, low availability of monosaccharides like glucose and in absence of a
326 living plant surface[29,49]. Although sugars are present as poly- and monosaccharides in the

327 soil[50], our results demonstrate that the resulting concentrations are not sufficient to inhibit
328 mycosporine generation and to break the dormancy of falcate conidia. Despite the
329 identification of mycosporines as germination regulator for *C. graminicola* in the 1990s[49], the
330 biosynthesis and its regulation is unclear until today, demanding for future studies unveiling
331 this critical part of the maize anthracnose fungus.

332 Taken together, our results indicate that oval and falcate conidia are adapted for distinct
333 phases of the overall maize anthracnose cycle. In this cycle, oval conidia serve as primary
334 inocula starting a root infection process enabled by fast germination in soil and chemotropic
335 sensing of the host roots. Outgoing from primary root infection, the maize plant gets infected
336 systemically and acervuli are developed on leaves giving birth to falcate conidia. Those are
337 dispersed by wind and rain to other maize plants, spreading the disease in the field via
338 continuous leaf infections. To our knowledge, such a specialization of two different asexual
339 spore types for host infection was not reported for any other plant pathogenic fungus. However,
340 it could be an unexplored adaptation strategy in many species and of outmost relevance for
341 successful crop protection.

342

343 Online Methods

344 Strains, growth conditions, and collection of spores

345 The sequenced *C. graminicola* (Ces.) G.W. Wilson (teleomorph *Glomerella graminicola* D. J.
346 Politis[51]) wildtype strain M2 (also referred to as M1.001) was used[52]. Falcate conidia production
347 of *C. graminicola* was induced by growth on oat meal agar (OMA; 1L contains 50 g ground oat
348 flakes (Alnatura, Bioland)) and the exposition to red (660-665 nm) and blue (450-455 nm) light
349 in a ratio 3:1 at 23°C[29]. After 14-21 d collection of falcate conidia with 0.02% Tween 20 solution.
350 For the generation of oval conidia, liquid complex medium containing sucrose (CMS, 1%
351 glucose, 0.1% yeast extract, 0.1% peptone, 0.5 M sucrose, 5.3 mM $Ca(NO_3)_2$) 0.073 mM
352 KH_2PO_4, 1.04 mM $MgSO_4$, 0.46 mM NaCl) was inoculated with 50 µl falcate spore stock
353 solution or mycelial plugs. After germination induction at 23°C for 2-3 d (80 rpm), further
354 incubation took place for 5-8 d without agitation in darkness. Oval conidia are collected by
355 filtration through Miracloth (Merck-Millipore, Darmstadt, Germany) followed by centrifugation
356 and a single washing step with demineralized water.

357 Generation of plasmids and *C. graminicola* strains

358 A ΔCgste3 deletion mutant and the complementation strain ΔCgste3::Cgste3 were generated
359 to analyze whether the a-pheromone receptor CgSte3 is involved in the sensing of maize root
360 exudates (MRE). Assembly of the corresponding plasmids was conducted using the NEBuilder
361 HiFi DNA Assembly Cloning Kit (New England Biolabs) according to the instruction manual.
362 All plasmids were verified using DNA hydrolysis and sequencing using appropriate enzymes
363 and primers. Oligonucleotides, strains and plasmids used are listed in supplementary tables
364 S1-S3.

365 As basis for homologous recombination in *C. graminicola*, the plasmid pCgste3_KO was
366 generated by the assembly of three PCR fragments into pJet1.2 (Thermo Scientific). The
367 fragments 5' *Cgste3* (Ste3_P_fw//Ste3_P_rv; 1,043 bp) and 3' *Cgste3* (Ste3_T_fw//Ste3_T_rv;
368 1031 bp) were amplified from *C. graminicola* genomic DNA. The *hph* cassette, mediating

369 resistance to hygromycine B, was generated using the plasmid pRS-hyg as template (hph-
370 f//hph-r; 1,417 bp)[53].

371 For ΔCgste3 complementation, the plasmid pCgste3_nat was constructed. The 5' and 3'
372 regions of *Cgste3* were amplified together with the *Cgste3* gene in a PCR using genomic DNA
373 of *C. graminicola* as template (Ste3_c_fw//Ste3_c_rv; 3,215 bp). As backbone for the assembly
374 reaction served pJet_nat linearized with *Eco*RV[30], resulting in a resistance to nourseothricin-
375 dihydrogen sulphate in *C. graminicola* strains transformed with this plasmid.

376 Prior to transformations in *C. graminicola*, the plasmids pCgste3_KO and pCgste3_nat were
377 linearized using the enzymes *Nae*I and *Sca*I, respectively. Oval conidia of CgM2
378 (transformation of pCgste3_KO) or ΔCgste3 (transformation of pCgste3_nat) served as basis
379 for the generation of protoplasts as described previously[33]. After transformation, regenerating
380 protoplasts were selected on medium containing hygromycin B (500 µg/ ml, transformation of
381 pCgste3_KO) or nourseothricin-dihydrogen sulphate (70 µg/ ml, transformation of
382 pCgste3_nat). To obtain homokaryotic strains, single spore isolations were performed of
383 antibiotic-resistant and PCR-verified primary transformants[30].

384 Single spore isolates of ΔCgste3 were verified by Southern Blot analyses. Hydrolysis of
385 genomic DNA (gDNA) was performed with the enzyme *Nae*I (Thermo Scientific). For the
386 visualization of successful deletion of the *Cgste3* gene via homologous recombination, the 3'
387 region of *Cgste3* was amplified in a PCR reaction (Ste3_T_fw//Ste3_T_rv; 1,031 bp) and used
388 as specific probe in the following hybridization reaction (expected sizes: CgM2 2,196 bp,
389 ΔCgste3 7,896 bp, Figure S7). Re-integration of *Cgste3* into the ΔCgste3 deletion strain was
390 tested via PCR using the primer pair Ste3_fw//Ste3_rv (1,136 bp), verifying ΔCgste3::Cgste3
391 primary transformants and single spore isolates (Figure S8).

392 Root infection analyses

393 Two different methods were applied for all experiments, to study different aspects of
394 *C. graminicola* root infection of the *Zea mays* cultivar 'Mikado' (KWS SAAT SE, Einbeck,
395 Germany). Unless otherwise stated, incubation of plants was performed in a PK 520 WLED
396 plant chamber (Poly Klima Climatic Growth System, Freising, Germany) using a day/night
397 cycle of 12 h 26°C/12 h 18°C. The strains CgM2, CgM2::RH2B, expressing tdTomato labeled
398 histone 2B[29], and ΔCgste3 were used for root infection experiments.

399 Infection by a root-dipping technique

400 *Z. mays* roots were dipped in conidial suspensions when 5 d old as described previously by
401 Sukno et al. 2008 to examine the general ability of *C. graminicola* to infect roots[28]. Early (4 dpi)
402 or late (21 dpi) developed symptoms were examined microscopically. First, seeds of *Z. mays*
403 were surface sterilized in 10% sodiumhypochlorite for 10 min and incubated for 5 d in rectangle
404 petri dishes (82.9923.422, Sarstedt, Nümbrecht, Germany) on wet blotting paper (BF2 580x
405 600mm, Sartorius, Göttingen, Germany). Incubation took place in darkness using standard
406 plant growing conditions. The developed roots of 5 d old seedlings were soaked in solutions
407 of either oval or falcate conidia of CgM2::RH2B (c= 10^7 x ml^{-1}) for 1h at 100 rpm. As mock
408 control, roots were soaked in sterile demineralized water. For follow up microscopic
409 examinations, the *C. graminicola* coated plants were incubated on wet blotting paper for 4 d.
410 2 ml of demineralized water was added on the blotting paper after 2 d to prevent drought stress
411 induction. For analysis of symptom development after 21 d, seedlings were planted in 40 g
412 vermiculite (Vermiculite Palabora, grain size 2-3 mm, Isola Vermiculite GmbH, Sprockhövel,

413 Germany) after dipping. The pots were covered with disposal plastic bags and sealed
414 (Sarstedt, Nümbrecht, Germany). After 21 d of incubation, length and biomass of the above-
415 ground plants were determined, pictures of the symptom development were taken and
416 spreading into stem material assessed with real-time PCR (2.3.3).

417 Root infections outward of *C. graminicola* enriched vermiculite

418 Maize seeds were planted in 40 g of vermiculite (Vermiculite Palabora, grain size 2-3 mm,
419 Isola Vermiculite GmbH, Sprockhövel, Germany) enriched with oval conidia of CgM2 or
420 ΔCgste3 in a concentration of 7.5 x 10^4 x $ml^{-}1$, to simulate a root infection outgoing from *C.*
421 *graminicola* conidia present in agricultural soil. As mock control, seeds were sown in
422 vermiculite mixed with water. To ensure high humidity, the pots were sealed in disposal plastic
423 bags (Sarstedt, Nümbrecht, Germany). 21 dpi, length and biomass of the above-ground plant
424 was determined and stem samples taken for follow up real-time PCR (2.3.3).

425 Identification of *C. graminicola in planta* via real-time PCR

426 We developed a PCR-based identification method, to monitor the spreading of *C. graminicola*
427 from infected roots into plant stems. First, oligonucleotides (ITS_P4_fw and ITS_P9_rv) were
428 designed to bind to *C. graminicola*-specific sequences of ITS1 and ITS2 flanking 5.8S rRNA.
429 The primer pair amplifies a 339 base pair fragment on a template of *C. graminicola* gDNA.
430 Importantly, no amplicons were generated using gDNA from the fungi *S. macrospora,*
431 *Verticillium dahliae, Verticillium longisporum, Aspergillus fumigatus* and *Aspergillus nidulans*
432 as template in verification PCRs (Figure S3 a). Therefore, the primer pair was used in the real-
433 time PCR on *C. graminicola*-infected plant material. To obtain template DNA, stems from
434 infected plants obtained by the infection protocols described, were surface sterilized for 2 min
435 in 10% sodium hypochlorite solution. From the lower part, 0.5 cm of stem were discarded. The
436 following 2 cm of the plant stems were frozen in liquid nitrogen and stored at -80°C (Figure S3
437 B). The collected stem samples were grinded in liquid nitrogen to fine powder. 500 µl extraction
438 buffer (Tris HCl pH 8.5 10 ml (from 1 M stock solution) EDTA 2.5 ml (from 0.5 M stock solution)
439 SDS 3.125 ml (from 8% stock solution) NaCl 6.25 ml (from 2 M stock solution) demineralized
440 water) was added to each sample. At this step, the plasmid peGFP-Cgatg8_gen (0.05 ng/µl)
441 was added as an external standard for DNA losses during gDNA extraction. Further extraction
442 was achieved with 8 M potassium acetate and chloroform. The DNA was precipitated with ice-
443 cold isopropanol at -20°C for 2 h to overnight. The resulting pellet was resuspended in 50 µl
444 demineralized water plus 2 µl RNase. Real-time PCR was performed with the MESA GREEN
445 qPCR MasterMix Plus for SYBR Assay (Eurogentec, Seraing, Belgium). For detection, a CFX
446 Connect Real Time PCR Detection System (Bio-Rad Laboratories, Hercules, CA, USA) was
447 used. The external standard plasmid peGFP-Cgatg8_gen served as template for amplification
448 with the oligonucleotide pair GFP-f and GFP-r. Follow up DNA sequencing and BLAST
449 analyses verified the identity of the obtained fragment outgoing from gDNA of the stem
450 samples as originating from *C. graminicola* (Figure S3 c).

451 Microscopy

452 Light (differential interference contrast (DIC)) and fluorescence microscopy was performed
453 with the AxioImager M1 microscope (Zeiss, Jena, Germany). The Photometrix coolSNAP HQ
454 camera (Roper Scientific, Photometrics, Tucson, AZ, USA) was used to capture images and
455 processing was performed with the ZEISS ZEN software (version 2.3, Zeiss). Visualization of
456 expressed red fluorescent CgM2::RH2B was achieved by a 49005 Chroma filter set (exciter

457 ET545/30x, emitter ET620/60 and beam splitter T570LP). At least three biological replicates
458 were performed for each experiment.

459 Generation and chemical analysis of maize root exudate

460 Roots of four 9 d old maize plants grown in vermiculite (Vermiculite Palabora, grain size 2-3
461 mm, Isola Vermiculite GmbH, Sprockhövel, Germany) under standard conditions to generate
462 MRE. The roots were rinsed and placed in 40 ml demineralized water. After incubation for
463 further 5 d in a plant chamber, MRE was sterile filtrated with a 0.45 µm filter (86.1197, Sarstedt,
464 Nümbrecht, Germany).

465 An HPLC/MS analysis was applied to analyze MRE for probable bioactive substances. The
466 MRE was extracted with ethyl acetate (1:1) or chloroform:methanol (1.8:2:2). Prior to
467 HPLC/MS analysis, the samples were solved in 500 µl methanol. The received suspensions
468 were centrifuged at 13000 rpm for 10 min at 4°C to remove unsolved particles. 400 µl of the
469 supernatants were transferred to LC-MS glass vials. A Q-Exactive™ Focus orbitrap mass
470 spectrometer coupled to a Dionex Ultimate 3000 HPLC (Thermo Fisher Scientific) was used
471 for analysis. HPLC was carried out using a Acclaim™ 120, C_{18}, 5 µm, 120 Å, 4.6 x 100 mm. 5
472 µl of each sample was injected for analysis. Running phase was set as a linear gradient from
473 5 - 95% (v/v) acetonitrile/0.1 formic acid in 20 min, plus 10 min with 95% (v/v) acetonitrile/0.1
474 formic acid) with a flow rate of 0.8 ml/min at 30°C in addition. The measurements were
475 performed in positive and negative modes with a mass range of 70-1050 m/z. UV/Vis spectra
476 were recorded with a Thermo Scientific™ Dionex™ UltiMate™ 3000 Diode Array Detector.
477 MS2 data were recorded at a HCD energy of 35 eV. For data analysis the software FreeStyle™
478 1.4 (Thermo Fisher Scientific) and the database "Dictionary of Natural Products" were used.

479 For the HPLC fractionation of MRE, the extraction of 8.5 L of exudate was performed with an
480 equal amount of ethyl acetate. The solvent was evaporated in a rotary evaporator and the
481 resulting extract (387 mg) applied onto a preparative HPLC-system. HPLC purification was
482 performed on a Shimadzu LC system equipped with a LC-20AP pump, an FCV-200AL valve,
483 a CBM-40 controller and an FRC-10A fraction collector. Separations were done on a
484 preparative reversed phase C18 column (Waters Sunfire C18, particle size 5 µm, 19 x 250mm)
485 and a semipreparative reversed phase C18 column (Waters Sunfire C18, particle size 5 µm,
486 10 x 250mm) at room temperature. A linear gradient starting from 1% 0.1% TFA and 99%
487 Acetonitrile to 100% Acetonitrile in 20 min, then maintaining 100% Acetonitrile for 3 min and
488 an additional equilibration time of 7 min was used at a flow rate of 17.1 ml/min. Injection volume
489 of sample solution was 1 ml. Volume of collected fractions were 3 ml. A Shimadzu SPD-M40A
490 diode array detector was used from 200-800 nm for recording of spectra and detection of
491 separated secondary metabolites at 210, 250, 300, 350 and 400 nm. Data and spectra were
492 analyzed using the software LabSolution 5.110. LC-ESI-MS analysis was performed on a
493 Shimadzu LC system equipped with two LC-40D pumps, a DGU-405 degassing unit, a SIL
494 40C autosampler, a SCL-40 controller and a CTO-40C column oven. Mass Analysis was
495 performed with a single quadrupole LCMS-2020 system. Separations were done on an
496 analytical reversed phase C18 column (Macherey Nagel, Nucleoshell RP18, particle size 2.7
497 µm, 2 x 100mm) at 40°C. A gradient starting from 95% 0,1% FA and 5% Acetonitrile with a
498 holding time of 2 min to 100% Acetonitrile in 6 min, then maintaining 100% Acetonitrile for 2
499 min and an additional equilibration time of 4 min was used at a flow rate of 0.3 ml/min. Injection
500 volume of sample solution was 1 µl. A Shimadzu SPD-M40A diode array detector was used
501 from 200-800 nm for recording of spectra and detection of secondary metabolites at 210 nm,
502 250 nm, 300 nm, 350 nm, 400 nm, 450 nm and 500 nm. A single quadrupole LCMS System-

2020 (Shimadzu) with ESI was used with following parameters: Scan mode, positive and negative, starting from 150 to 1000 m/z with acquisition time from 2 to 10 min. DL temperature 250 °C, nebulizing gas flow 1.5 L/min, drying gas flow 10 L/min and the temperature of the heat block was 200 °C. Data and spectra were analyzed using the software LabSolution 5.109.

Chemotropic assay

Quantification of chemotropic growth of different *C. graminicola* germlings derived from oval and falcate conidia, towards MRE, different MRE fractions, oryzalexin D, dihydrotanshinone I, phytane, and attractants within MRE, was performed after 6h of incubation using a 3D printed device as described previously[32,33]. From raw data, the chemotropic index was calculated, showing the difference of chemotropic attraction compared to non-stimulating conditions[15].

Analysis of *C. graminicola* germination patterns

For quantification of germination in soil, 1.875 ml spores solution (c = 1.5*10^6) of either oval or falcate conidia was mixed in 5 ml vermiculite or soil (I)-vermiculite (mix of soil (I) (Einheitserde Classic, Patzer Erden GmbH, Sinntal-Altengronau, Germany) and vermiculite (Vermiculite Palabora, grain size 2-3 mm, Isola Vermiculite GmbH, Sprockhövel, Germany), ratio 4+1) mixture. After incubation (0 h, 6 h, 24 h, 48 h, 10 d), 2.5 ml water was added to wash out remaining spores. To access the rate of remaining not-germinated spores, those were quantified in a Neubauer counting chamber. 50 µl spore solution (c = 10^6 x ml^{-1}) was dropped on water agar (1L contains 10 g agarose, 10 g serva agar, 2.1 g $NaNO_3$). After evaporation of the liquid, 20µl MRE was added on top of the spores to analyze the effect of MRE on germination. Microscopy of germination behavior of falcate conidia in soil was performed after 24 h incubation in either vermiculite, soil (I)-vermiculite (4+1) mixture or soil (II) -compost soil-sand mixture (mix of soil (II) (Einheitserde Type P 25, Archut Erdenwerk, Vechta, Germany; compost soil, steamed for 24 h at 105°C, botanical garden, Göttingen, Germany; sand, grain size 0-2mm, August Oppermann Kiesgewinnungs- und Vertriebs-GmbH, Northeim, Germany; ratio 3+3+1).

Statistics

The T-test for unequal variances was used for all experiments in this study[54].

Acknowledgements

We thank Gabriele Beyer, Gertrud Stahlhut and Christiane Grünewald for excellent technical assistance. Genomic DNA of *Verticillium dahliae* and *Verticillium longisporum* was provided by Rebekka Harting. Genomic DNA of *Aspergillus fumigatus* and *Aspergillus nidulans* was provided by Anja Strohdiek. This work was funded by the Deutsche Forschungsgemeinschaft (Bonn-Bad Godesberg). Grants were provided to D.E.N. (project NO 1230/3-1 (447175909 and to D.E.N. and G.B. (IRTG 2172: PRoTECT program (GRK 2172, project number 273134146)).

Contributions

Establishment of maize root infections was done by A.Y.R., C.S. and D.E.N. and performed by A.Y.R. and C.S.. Quantification of chemotropic growth was done by A.Y.R. and D.E.N.. Maize root exudate was generated by A.Y.R. and D.E.N., chemically extracted by A.Y.R. and D.E.N. and analyzed by HPLC/MS analyses by J.G., C.S. and L.A.. Fractionation of maize root exudate was done by L.A.. Generation of deletion mutant and complementing strain was performed by D.E.N.. Real-time PCR and germination analyses were established and performed by A.Y.R.. A.Y.R. and D.E.N. wrote this manuscript with invaluable assistance from G.B. and S.P. and the other co-authors.

References

1 Strange, R. N. & Scott, P. R. Plant disease: a threat to global food security. *Annual Review of Phytopathology* **43**, 83-116 (2005).

2 Fisher, M. C. *et al.* Emerging fungal threats to animal, plant and ecosystem health. *Nature* **484**, 186-194 (2012).

3 Silva, R. N. *et al.* Trichoderma/pathogen/plant interaction in pre-harvest food security. *Fungal biology* **123**, 565-583 (2019).

4 Chaloner, T. M., Gurr, S. J. & Bebber, D. P. Plant pathogen infection risk tracks global crop yields under climate change. *Nature Climate Change* **11**, 710-715 (2021).

5 Zhang, W. Global pesticide use: Profile, trend, cost/benefit and more. *Proceedings of the International Academy of Ecology and Environmental Sciences* **8**, 1-27 (2018).

6 Kou, Y. & Naqvi, N. I. in *Seminars in cell & developmental biology.* 84-92 (Elsevier).

7 Okubara, P. A. & Paulitz, T. C. Root defense responses to fungal pathogens: a molecular perspective. *Root physiology: from gene to function* **274**, 215-226 (2005).

8 Steinkellner, S., Mammerler, R. & Vierheilig, H. Microconidia germination of the tomato pathogen *Fusarium oxysporum* in the presence of root exudates. *Journal of Plant Interactions* **1**, 23-30 (2005).

9 Narula, N., Kothe, E. & Behl, R. K. Role of root exudates in plant-microbe interactions. *Journal of Applied Botany and Food Quality* **82**, 122-130 (2009).

10 Vives-Peris, V., De Ollas, C., Gómez-Cadenas, A. & Pérez-Clemente, R. M. Root exudates: from plant to rhizosphere and beyond. *Plant Cell Reports* **39**, 3-17 (2020).

11 Deacon, J. & Donaldson, S. Molecular recognition in the homing responses of zoosporic fungi, with special reference to *Pythium* and *Phytophthora*. *Mycological Research* **97**, 1153-1171 (1993).

12 Donaldson, S. & Deacon, J. Effects of amino acids and sugars on zoospore taxis, encystment and cyst germination in *Pythium aphanidermatum* (Edson) Fitzp., P. catenulatum Matthews and *P. dissotocum* Drechs. *New Phytologist* **123**, 289-295 (1993).

13 Ruttledge, T. R. & Nelson, E. B. Extracted fatty acids from *Gossypium hirsutum* stimulatory to the seed-rotting fungus, *Pythium ultimum*. *Phytochemistry* **46**, 77-82 (1997).

14 Tyler, B. M. Molecular basis of recognition between *Phytophthora pathogens* and their hosts. *Annual review of phytopathology* **40**, 137-167 (2002).

15 Turrà, D., El Ghalid, M., Rossi, F. & Di Pietro, A. Fungal pathogen uses sex pheromone receptor for chemotropic sensing of host plant signals. *Nature* **527**, 521-524 (2015).

16 Sridhar, P. S. *et al.* Ste2 receptor-mediated chemotropism of *Fusarium graminearum* contributes to its pathogenicity against wheat. *Scientific Reports* **10**, 10770 (2020).

17 Vangalis, V. *et al.* Components of TOR and MAP kinase signaling control chemotropism and pathogenicity in the fungal pathogen *Verticillium dahliae*. *Microbiological Research* **271**, 127361 (2023).

18 Lagopodi, A. L. *et al.* Novel aspects of tomato root colonization and infection by *Fusarium oxysporum* f. sp. *radicis-lycopersici* revealed by confocal laser scanning microscopic analysis using the green fluorescent protein as a marker. *Molecular Plant-Microbe Interactions* **15**, 172-179 (2002).

19 Zhao, Y.-L., Zhou, T.-T. & Guo, H.-S. Hyphopodium-specific VdNoxB/VdPls1-dependent ROS-Ca2+ signaling is required for plant infection by *Verticillium dahliae*. *PLoS pathogens* **12**, e1005793 (2016).

20 Marcel, S., Sawers, R., Oakeley, E., Angliker, H. & Paszkowski, U. Tissue-adapted invasion strategies of the rice blast fungus *Magnaporthe oryzae*. *The Plant Cell* **22**, 3177-3187 (2010).

21 Dufresne, M. & Osbourn, A. E. Definition of tissue-specific and general requirements for plant infection in a phytopathogenic fungus. *Molecular Plant-Microbe Interactions* **14**, 300-307 (2001).

22 Bergstrom, G. C. & Nicholson, R. L. The biology of corn anthracnose: knowledge to exploit for improved management. *Plant disease* **83**, 596-608 (1999).

23 from:, C. P. N. T. Y. L. C. R. & https://cropprotectionnetwork.org/crops/cor.

24 Belisário, R., Robertson, A. E. & Vaillancourt, L. J. Maize anthracnose stalk rot in the genomic era. *Plant Disease* **106**, 2281-2298 (2022).

25 Zhang, H., Wu, Z., Wang, C., Li, Y. & Xu, J.-R. Germination and infectivity of microconidia in the rice blast fungus *Magnaporthe oryzae*. *Nature communications* **5**, 4518 (2014).

26 Ohara, T., Inoue, I., Namiki, F., Kunoh, H. & Tsuge, T. *REN1* is required for development of microconidia and macroconidia, but not of chlamydospores, in the plant pathogenic fungus *Fusarium oxysporum*. *Genetics Society of America* **166**, 113-124 (2004).

27 Panaccione, D. G., Vaillancourt, L. J. & Hanau, R. M. Conidial dimorphism in *Colletotrichum graminicola*. *Mycologia* **81**, 876-883 (1989).

28 Sukno, S. A., García, V. n. M., Shaw, B. D. & Thon, M. R. Root infection and systemic colonization of maize by Colletotrichum graminicola. *Applied environmental microbiology* **74**, 823-832 (2008).

29 Nordzieke, D. E. *et al.* Specialized infection strategies of falcate and oval conidia of *Colletotrichum graminicola*. *Fungal Genetics Biology* **133**, 103276 (2019).

30 Nordzieke, D. E. Hyphal Fusions Enable Efficient Nutrient Distribution in *Colletotrichum graminicola* Conidiation and Symptom Development on Maize. *Microorganisms* **10**, 1146 (2022).

31 Nordzieke, D. E., Fernandes, T. R., El Ghalid, M., Turrà, D. & Di Pietro, A. NADPH oxidase regulates chemotropic growth of the fungal pathogen *Fusarium oxysporum* towards the host plant. *New Phytologist* **224**, 1600-1612 (2019).

32 Schunke, C., Pöggeler, S. & Nordzieke, D. E. A 3D printed device for easy and reliable quantification of fungal chemotropic growth. *Frontiers in Microbiology* **11**, 584525 (2020).

33 Groth, A., Schunke, C., Reschka, E. J., Pöggeler, S. & Nordzieke, D. E. Tracking fungal growth: Establishment of Arp1 as a marker for polarity establishment and active hyphal growth in filamentous ascomycetes. *Journal of Fungi* **7**, 580 (2021).

34 Mafu, S. *et al.* Discovery, biosynthesis and stress-related accumulation of dolabradiene-derived defenses in maize. *Plant physiology* **176**, 2677-2690 (2018).

35 Sharma, T. *et al. Fusarium graminearum* Ste3 G-Protein Coupled Receptor: A Mediator of Hyphal Chemotropism and Pathogenesis. *Msphere* **7**, e00456-00422 (2022).

36 Wilson, A. M., Lelwala, R. V., Taylor, P. W., Wingfield, M. J. & Wingfield, B. D. Unique patterns of mating pheromone presence and absence could result in the ambiguous sexual behaviors of *Colletotrichum* species. *G3* **11**, jkab187 (2021).

37 Li, X.-g. *et al.* The composition of root exudates from two different resistant peanut cultivars and their effects on the growth of soil-borne pathogen. *International Journal of Biological Sciences* **9**, 164 (2013).

38 Eze, C. Root Exudate Effect on Germination and Mycelial Growth of Sclerotia of *Sclerotium rolfsii* Sacc. *Bio-Research* **8**, 626–628 (2010).

39 Zhang, X. *et al.* Transcriptomic analysis of gene expression of Verticillium dahliae upon treatment of the cotton root exudates. *BMC genomics* **21**, 1-25 (2020).
40 Lanoue, A. *et al.* De novo biosynthesis of defense root exudates in response to *Fusarium* attack in barley. *New Phytologist* **185**, 577-588 (2010).
41 Mika, A., Boenisch, M. J., Hopff, D. & Lüthje, S. Membrane-bound guaiacol peroxidases from maize (*Zea mays* L.) roots are regulated by methyl jasmonate, salicylic acid, and pathogen elicitors. *Journal of Experimental Botany* **61**, 831-841 (2010).
42 Bindschedler, L. V. *et al.* Peroxidase-dependent apoplastic oxidative burst in Arabidopsis required for pathogen resistance. *The Plant Journal* **47**, 851-863 (2006).
43 Wen, F., VanEtten, H. D., Tsaprailis, G. & Hawes, M. C. Extracellular proteins in pea root tip and border cell exudates. *Plant physiology* **143**, 773-783 (2007).
44 Zhou, H., Hua, J., Li, H., Song, X. & Luo, S. Structurally diverse specialized metabolites of maize and their extensive biological functions. *Journal of Cellular Physiology* (2023).
45 Schmelz, E. A. *et al.* Identity, regulation, and activity of inducible diterpenoid phytoalexins in maize. *Proceedings of the National Academy of Sciences* **108**, 5455-5460 (2011).
46 Hiraga, S., Sasaki, K., Ito, H., Ohashi, Y. & Matsui, H. A large family of class III plant peroxidases. *Plant Cell Physiology* **42**, 462-468 (2001).
47 Kidwai, M., Ahmad, I. Z. & Chakrabarty, D. Class III peroxidase: An indispensable enzyme for biotic/abiotic stress tolerance and a potent candidate for crop improvement. *Plant cell reports* **39**, 1381-1393 (2020).
48 Huffaker, A. *et al.* Novel acidic sesquiterpenoids constitute a dominant class of pathogen-induced phytoalexins in maize. *Plant physiology* **156**, 2082-2097 (2011).
49 Leite, B. & Nicholson, R. L. Mycosporine-alanine: A self-inhibitor of germination from the conidial mucilage of *Colletotrichum graminicola*. *Experimental mycology* **16**, 76-86 (1992).
50 Gunina, A. & Kuzyakov, Y. Sugars in soil and sweets for microorganisms: Review of origin, content, composition and fate. *Soil Biology & Biochemistry* **90**, 87-100 (2015).
51 Forgey, W., Blanco, M. & Loegering, W. Differences in pathological capabilities and host specificity of *Colletotrichum graminicola* on *Zea mays*. *Plant Disease Reporter* **62**, 573-576 (1978).
52 O'Connell, R. J. *et al.* Lifestyle transitions in plant pathogenic *Colletotrichum* fungi deciphered by genome and transcriptome analyses. *Nature genetics* **44**, 1060-1065 (2012).
53 Bloemendal, S. *et al.* A homologue of the human STRIPAK complex controls sexual development in fungi. *Molecular microbiology* **84**, 310-323 (2012).
54 Ruxton, G. D. The unequal variance t-test is an underused alternative to Student's t-test and the Mann–Whitney U test. *Behavioral Ecology* **17**, 688-690 (2006).